LIMNOLOGY and OCEANOGRAPHY

ASLO

Limnol. Oceanogr. 9999, 2024, 1–11

doi: 10.1002/lno.12584

Sight and blindness: The relationship between ostracod eyes, water depth, and light availability in the Arctic Ocean

Jingwen Zhang,[1,2*] Moriaki Yasuhara,[1,2*] Chih-Lin Wei,[3] Skye Yunshu Tian,[1,2] Kyawt K. T. Aye,[1,2] Laura Gemery,[4] Thomas M. Cronin,[4] Peter Frenzel,[5] David J. Horne[6,7]

[1]School of Biological Sciences, Area of Ecology and Biodiversity, Swire Institute of Marine Science, Institute for Climate and Carbon Neutrality, and Musketeers Foundation Institute of Data Science, The University of Hong Kong, Kadoorie Biological Sciences Building, Hong Kong, China
[2]State Key Laboratory of Marine Pollution, City University of Hong Kong, Hong Kong, China
[3]Institute of Oceanography, National Taiwan University, Taipei, Taiwan
[4]U.S. Geological Survey, Florence Bascom Geoscience Center, Reston, Virginia, USA
[5]Institute of Geosciences, Friedrich Schiller University of Jena, Jena, Germany
[6]School of Geography, Queen Mary University of London, London, UK
[7]Earth Sciences Department, The Natural History Museum, London, UK

Abstract

Eye loss has been a long-standing interest in evolutionary biology. Many organisms that inhabit environments without light penetration, for example the deep sea, exhibit eye loss and thus become blind. However, water-depth distribution of eyes in marine organisms is poorly understood. Ostracods are widely distributed crustaceans, and many sighted marine ostracods have eye tubercles (lenses) on their shells. Since eye tubercles are visible on the shells illustrated in much literature, it is easy to determine their presence or absence via a literature survey. Here, we used a large Arctic-wide ostracod census dataset (Arctic Ostracode Database) to calculate the eye index (the percentage of species with eyes), and compare them with water depth and light availability. As water depth increases, eye index values decrease and become constantly zero in water deeper than 1000 m. Similar decline of sighted species with increasing depth is also known in isopods and amphipods, suggesting that it may be common in other crustaceans and perhaps in deep-sea organisms in general. We also show that eye index values increase as light availability increases. This study is the first to quantify how distributions of sighted and blind species change with light availability, giving baseline information on vision in the deep sea.

The evolutionary reduction or loss of eyes is a well-known feature of metazoans adapted to low-light or aphotic environments such as caves and the deep ocean floor (Raupach et al. 2009; Porter and Sumner-Rooney 2018). In the permanent absence of available light, eye loss is considered to be an adaptation driven by directional selective pressure resulting from the altered balance in the trade-off between the benefits and energy expenditure of eyes in an organism (Niven and Laughlin 2008; Sumner-Rooney et al. 2016). Theoretical considerations suggest that, in marine organisms, selective pressure might increase eye efficiency with decreasing light availability (with increasing water depth) up to a threshold of very low or no light, beyond which the selective pressure would be reversed in favor of eye reduction and loss. However, only a few studies have investigated how sighted and blind organisms are distributed along oceanic light availability gradients. A pioneering study using a large dataset of benthic marine isopod distribution (Menzies et al. 1968) demonstrated that the percentage of blind taxa increases with increasing water depth (although eye-bearing species still occur at depths well below the limits of visible light penetration) and also varies with latitude (poleward emergence of blind abyssal genera into shallow water). A similar strong correlation between blindness and depth has been recognized in marine amphipods (Thurston and Bett 1993) and gastropods (Williams et al. 2022).

*Correspondence: alex1999@connect.hku.hk; moriakiyasuhara@gmail.com; yasuhara@hku.hk

Author Contribution Statement: J.Z. and M.Y. designed the research. J.Z., C.-L.W., M.Y., L.G., D.J.H., T.M.C., S.Y.T., and K.K.T.A. performed the research. J.Z., C.-L.W., and M.Y. analyzed the data. J.Z., M.Y., D.J.H., C.-L.W., and P.F. wrote the paper with intellectual contributions from all authors.
J.Z., M.Y., and C.-L.W. contributed equally to this study.

Reviewing major evolutionary drivers of eye loss, Sumner-Rooney (2018) highlighted the future research importance of comparisons among multiple habitats but considered the identification of candidate systems (i.e., taxa) for study to be a major obstacle, observing that relatively few taxonomic groups have made both shallow to deep water and surface to subterranean habitat transitions in multiple lineages. Ostracod crustaceans are one such group, with the added benefit of a rich fossil record (*see*, e.g., Benson 1984; Danielopol et al. 1996; Syme and Oakley 2012), to address the research question how sighted and blind organisms are distributed along large-scale gradients of water depth and, thus, oceanic light availability from shallow-marine continental shelf to deep sea.

Podocopid ostracod eyes are examples of crustacean "naupliar eyes" that typically comprise three ocelli, i.e., two lateral ocelli and a median ventral ocellus lying between them, that are situated close to the front of the dorsal region (Tanaka 2005, 2006; Kaji and Tsukagoshi 2010). Eye tubercles are externally visible semi-globular structures of the calcareous shell, one in each of the two valves, situated over and forming a lens that focuses light onto the underlying lateral ocelli, and often associated with internal ocular sinuses in the inner surfaces of the valves (Tanaka 2005, 2006). Naupliar eyes are generally incapable of forming images but in at least one podocopid ostracod, a species of the freshwater cypridoidean genus *Notodromas*, the arrangement of a lens and a concave mirror in each ocellus enables a focused image in the retina (Anderson and Nilsson 1981); with current knowledge we can only speculate as to whether other podocopid ostracods have this ability, although it is noteworthy that many podocopids have cuticular lenses in the form of eye tubercles on the calcareous valves that must at least enhance the light-gathering ability of the lateral ocelli. The presence of eye tubercles, which being part of the calcareous valves are observable in fossil as well as living ostracods, may be considered to be a good indication that the ostracod possessing them is or was sighted. It is, at least, reasonable to assume that podocopid ostracod eyes are essentially light-detectors that are useful for orientation and perhaps the detection and avoidance of predators. The aforementioned *Notodromas* is a neuston-feeder that can be observed swimming inverted at the water-air interface (Smith and Kamiya 2014), a vulnerable location in which it is silhouetted against the daylight, but in which orientation its eyes are well positioned to detect predators approaching from beneath (D. J. Horne pers. observ. in microaquaria). We know of no evidence that podocopid eyes are used for more complex purposes such as locating prey or potential mates.

A pioneering study on marine podocopids is Benson's (1975) showing bathymetric distribution of "relative blindness among potentially sighted species." His result showed that the percentage of blind species increases with increasing water depth (Benson 1975), consistent with the isopod trend mentioned above (Menzies et al. 1968). The result also showed that "almost all species become blind in depths greater than 600 to 800 meters" (Benson 1975, text-fig. 23). However, any further methodological, sample, or locality details were not given in his study, including definition of blind and "potentially sighted" species, a list of "blind" and "sighted" species, and data treatment. Benson (1976, 1984) also discussed this topic but briefly without data. Nonetheless, studies on marine ostracod distributions tend to be based on calcareous shells instead of soft-body anatomy; these studies on ostracod vision are likely based on the presence/absence of eye tubercles. We tend to lack soft-anatomy-based information on the ostracod eye, except for a few detailed studies (e.g., Tanaka 2005, 2006) discussed below.

It is well known that deep-sea ostracods tend to be blind, assuming that the lack of eye tubercles means blind. For example, Benson (1984) reported that, among over 5000 Cretaceous and Paleocene ostracod specimens examined in the deep South Atlantic Ocean, none was found with eye tubercles. He listed the ostracod genera *Atlanticythere*, *Palaeoabyssocythereis*, *Phacorhabdotus*, and *Cytherella* and stated that all were blind. Yasuhara et al. (2015) depicted many deep-sea ostracod species without eye tubercles, using scanning electron microscopy.

An uncertainty is the existence of ostracod species with eyes but no easily recognizable ocular structure (e.g., eye tubercles) in their shells. Based on meticulous studies on podocopid ostracod eyes and related optical structures of calcareous shells, Tanaka (2005, 2006) found such species in families Bairdiidae, Candonidae, Darwinulidae, Paradoxostomatidae, and Bythocytheridae. Species of these families in general are likely sighted, but lack eye tubercles. Platycopids *Cytherella* and *Keijcyoidea* are also genera without eye tubercles but of which at least some shallow-water species are known to be sighted (Müller 1894; Tsukagoshi et al. 2006; Okada et al. 2008), but it remains possible (though difficult to verify) that deep-water species of *Cytherella* may be blind. Despite such uncertainty, it is well-established on the basis of living examples that ornamented ostracods of certain families (particularly the Hemicytheridae and Trachyleberididae) commonly have eyes and prominent eye tubercles in shallow-marine species (Tanaka 2005, 2006). In contrast, most deep-sea species lack eye tubercles, not only in these ornamented families (Yasuhara et al. 2015) but also in general (e.g., Yasuhara et al. 2009, 2021; Alvarez Zarikian 2015), indicating their blindness there. Thus, the presence/absence of eye tubercles can be used as an approximate proxy for sightedness/blindness.

Assuming that light availability is a key influence on the distribution of sighted and blind ostracods, the factors that determine light availability on the ocean floor must be considered. Studies of ostracod "depth-eyes" gradients have considered the primary factor to be light attenuation in water, which increases with depth and may also be influenced by suspended sediment in nearshore areas, or phytoplankton density in high-

productivity areas. According to Benson (1984, p. 121), the size (and possibly the clarity) of the eye tubercle "in general varies directly with the amount of light and therefore is water-mass turbidity and depth dependent". Considering the dimmest light levels likely to be detectable by ostracod eyes, Kontrovitz and Myers (1988) concluded that, in coastal waters, the limits of vision would be at depths from 28 to 85 m (depending on attenuation by turbidity), but as deep as 280 m in the clearest ocean water; however, their calculations appear to have been based on an assumption of the sun being more or less vertically above the ocean (i.e., as in tropical waters). Since they took no account of latitudinal variation, these values can probably be regarded as maxima and applicable only to low latitudes; it is noteworthy that even these estimated maximum possible depths are only (approximately) a half to a third of the depths at which Benson (1984) found that eye tubercles "disappeared."

Here we present the results of a study of marine benthic ostracods, which offer excellent potential for exploring present and past distributions along a "depth-eyes" gradient, because their calcified bivalved shells are readily preserved and can be extracted in abundance from surface sediment and core samples, and the shells of many sighted species display distinctive eye tubercles. We used a large census dataset of Arctic and Subarctic ostracods (Gemery et al. 2017; Cronin et al. 2021) to understand how the proportion of ostracod species with eye tubercles varies with depth and light penetration, and if ostracod "depth-eyes" gradients are consistent with those of other marine benthos such as isopods and amphipods, providing baseline information on macroecological-scale distribution of vision in the ocean.

Materials and methods

We used the Arctic Ostracode Database, which compiles the ostracod occurrence data of 96 taxa (mostly species with a few genus-level entries as "spp.") (47 genera) in 1574 surface sediment samples collected from 1933 to 2018, and covers the Beaufort Sea, Siberian Sea, Kara Sea, Laptev Sea, Chukchi Sea, Baffin Bay, Greenland Sea, and Barents Sea, and some adjacent subpolar regions (Gemery et al. 2017; Cronin et al. 2021). Among all species, *Acetabulastoma arcticum* is discarded since it lives in a sea ice habitat and cannot be regarded as a benthic species (Cronin et al. 2010). Hence, only 95 taxa are included in our analyses. They are all benthic podocopid ostracods, except a benthic myodocopid taxon *Polycope* spp. that does not have eye tubercles. Of 1574 sites, 11 sites are excluded due to lack of water depth information, and 802 sites are excluded due to their small sample size (< 50 specimens). The remaining 761 sites are used for data analysis (Fig. 1). We coded the presence/absence of eye tubercles for each species in the Arctic Ostracode Database by checking literature showing scanning electron microscope images, primarily Gemery et al. (2017) supplemented by Neale and Howe (1975), Benson et al. (1983), Penney (1993), Freiwald and Mostafawi (1998), Mackiewicz (2006), Schornikov and Zenina (2006), Stepanova (2006), and Yasuhara et al. (2014, 2015). We quantified ostracods with eye tubercles per sample using an "eye index" at species level. The eye index is the relative number of eyed species (i.e., number of eyed species divided by total number of species). For the purposes of this study, "eyed species" means species with eye tubercles.

We calculated the vertical transmittance of solar radiation in the visible domain, T_{vis} (z), using algorithms developed by

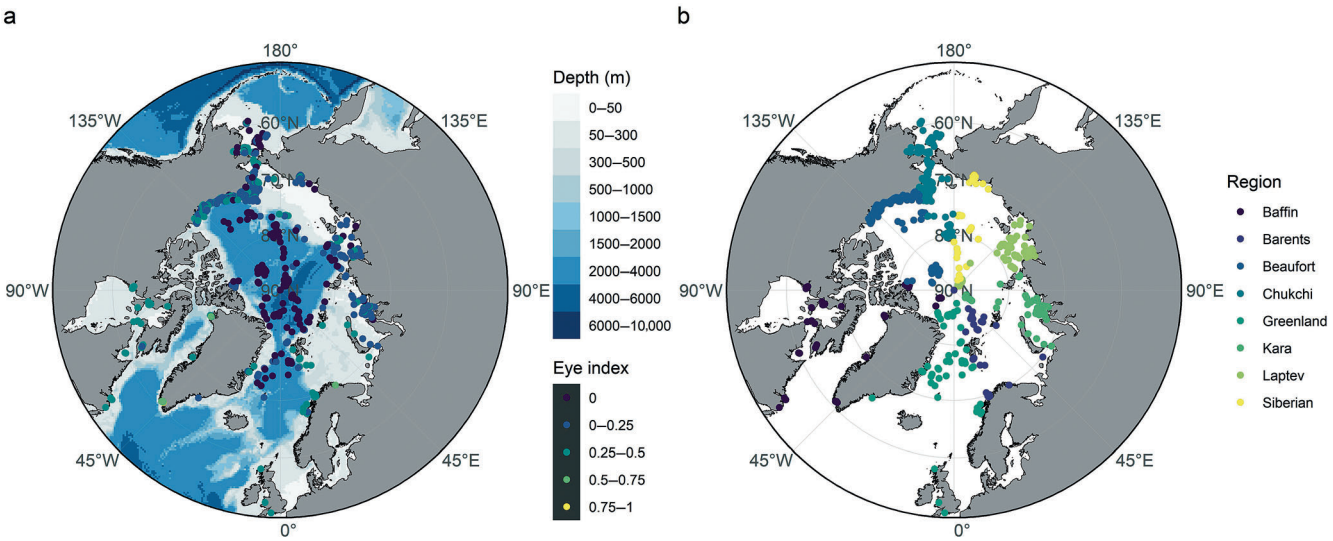

Fig. 1. Distribution map showing the location and eye index of each sample (**a**) and regional division of the Arctic Ostracode Database (**b**) in the Arctic Ocean. All analyses were performed using R Statistical Software (v4.0.3; R Core Team 2020). Water depth data and polar map were obtained from the Norwegian Polar Institute via the PlotSvalbard R package (v0.9.2; Mikko 2020). Plotting of data points relies on the ggplot2 R package (v3.4.2; Wickham 2016).

Lee et al. (2005). In short, the vertical transmittance T_{vis} (z) is the ratio downwelling solar radiation (for wavelengths in the range of 350–700 nm) at depth (z), thus determining the relative light availability in the visible domain. The vertical transmittance T_{vis} (z) is a negative exponential function of the attenuation coefficient (K_{vis}) for the downwelling solar radiation multiplied by the water depth. The attenuation coefficient K_{vis} was then estimated as a function of solar zenith angle and water's total absorption and particulate backscatter, derived from observations of ocean color. The detailed algorithms of the calculations and complete parameters are found in Lee et al. (2005). We then calculated the light availability (= the photosynthetically available radiation at depth, PAR (z)), by multiplying the photosynthetically available radiation at the surface with the vertical transmittance T_{vis} (z) at the sampling depth. The 4-km resolution, gridded total absorption at 488 nm (a488), backscatter at 488 nm (bb488), and photosynthetically available radiation from the MODIS Aqua entire mission composite climatology (averaging from 04 July 2002 to 30 September 2022) were downloaded from the NASA OceanColor Web L3 browser (https://oceancolor.gsfc.nasa.gov/l3/order/). The gridded absorbance and backscatter values at 488 nm were then extracted by sampling coordinates. For the coordinate outside of the grid coverages, we extracted the mean value from the surrounding grids within a 100-km radius buffer. The remaining coordinates not covered by the spatial grids or 100-km buffers are mostly under the permanent sea ice (between 84.3°N and 89.98°N); therefore, their vertical transmittance T_{vis} (z) is set to zero before analyses. We used generalized linear mixed-effect model (GLMM) with binomial distribution to fit a fixed factor, including water depth, vertical transmittance T_{vis} (z), photosynthetically available radiation at depth PAR (z), or latitude, to the eye index. The random factor of GLMMs used eight levels of ocean regions, including Beaufort Sea, Siberian Sea, Kara Sea, Laptev Sea, Chukchi Sea, Baffin Bay, Greenland Sea, and Barents Sea, to account for potential spatial autocorrelation. The data and codes to reproduce the figures and analyses are available in Zenodo open data repository (Zhang et al. 2024).

Results

Among 95 taxa in total, 21 from 11 genera have eye tubercles: *Acanthocythereis*, *Baffinicythere*, *Elofsonella*, *Finmarchinella*, *Hemicythere*, *Loxoconcha*, *Patagonacythere*, *Rabilimis*, *Roundstonia*, *Schizocythere*, and *Thaerocythere*. The majority of species with eye tubercles are from the families Hemicytheridae and Trachyleberididae, while those lacking eye tubercles are mainly from the family Cytherideidae (Fig. 2). The result shows that high eye index values mainly appear in lower latitude coastal areas, especially in Baffin Bay (Fig. 1). Ostracod eye index values exponentially decrease as the water depth increases. The eye index values decrease rapidly in the top 200 m and become almost constantly zero after the water depth exceeds 1000 m;

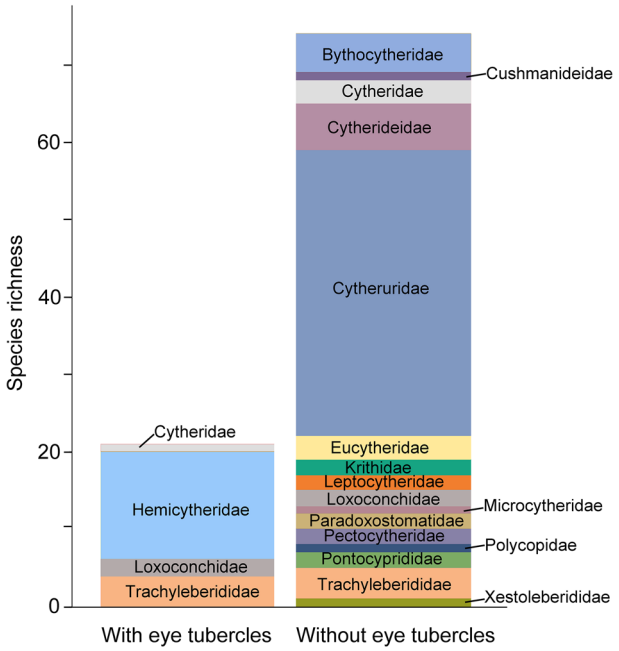

Fig. 2. Stacked bar chart showing species richness of ostracod families from the Arctic Ostracode Database with (left) and without (right) eye tubercles.

however, the relationship is noisy (Fig. 3). Although there are certain regional variations, in many regions such as Chukchi Sea, Baffin Bay, Greenland Sea, Barents Sea, and Kara Sea, high eye index values are concentrated in the top 200 m water depth (Fig. 4). In shallow depths (< ~ 100 m), the eye index values have large variation from 0 to ~ 0.8 (Fig. 3). Similarly, the eye index values significantly and exponentially decrease with decreasing light availability (PAR (z)) (Figs. 5, 6). The eye index also declines significantly with increasing latitudes (Fig. 7). Similar to the relationship between the eye index and water depth, these relationships are noisy with substantial regional variations (Figs. 3, 4, 6, 7). Especially in the range where the photosynthetically available radiation at depth (PAR (z)) is > 1, eye index varies from 0 to 0.8 (Fig. 6).

Discussion

We found a general pattern that ostracods with eye tubercles (i.e., eye index values) decrease with increasing water depth: it was still high in depths between ~ 100 and 200 m, and very low in depths deeper than 1000 m (Fig. 3). Results of this study support Benson's suggestion that complete loss of eye tubercles occurs at depths between ~ 600 and 800 m (Benson 1975). This depth range for eye loss is similar to those found in gastropods, isopods, and amphipods (Menzies et al. 1968; Thurston and Bett 1993; Williams et al. 2022). In our study, the eye index decreases as water depth increases, and a rapid change occurs at ~ 200 m, which is very similar to Menzies and others' result for isopods in polar regions

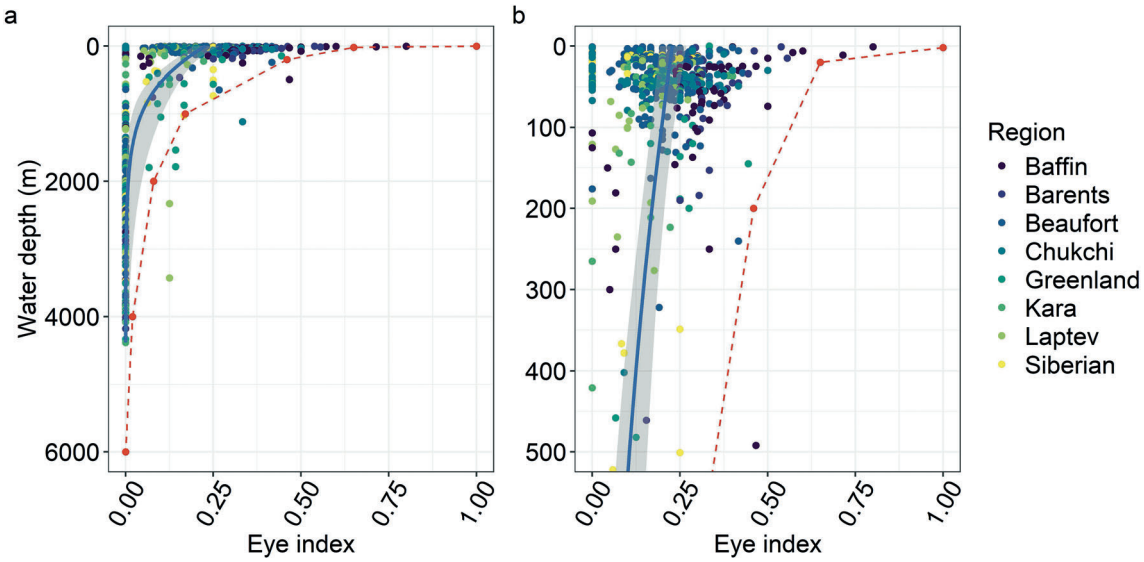

Fig. 3. Bathymetric distribution of eye index values in the Arctic Ocean. (**a**) The entire depth range, and (**b**) the samples from the top 500 m. Blue lines show significant relationships with 95% confidence intervals (shaded areas) based on the GLMM with binomial distribution. Red symbols and dashed lines show the isopod eye index from Menzies et al. (1968).

(Menzies et al. 1968; Fig. 3). While it is less clear in the GLMM curve, very high Eye Index values are concentrated in the top 200 m depths (Figs. 3, 4). This depth of change to ostracods without eye tubercles is very close to the physical limitation of vision with sunlight in podocopid Ostracoda, which is 280 m at a maximum (Kontrovitz and Myers 1988). This common trend among different groups of crustaceans makes sense, because light intensity is known to decline with increasing water depth to create an aphotic zone in marine environments deeper than 1000 m, which exceeds the threshold of vision for daylight (Denton 1990). The relatively few outlying records at greater depths (Figs. 3, 4) could represent taxa that only moved to deeper water relatively recently (many generations would be necessary for eye tubercle loss). A possible example of the transition to eye loss can be found in the podocopid genus *Eucytherura*, the type species of which (*Eucytherura complexa* [Brady, 1867]) appears to live at depths as shallow as 27 m and has distinct eye tubercles. The remarkably similar *Eucytherura delineata* Whatley and Eynon 1996 has closely similar valve morphology except for its eye tubercles which exist but are covered by reticulate ornament and presumably nonfunctional, and this species has been recorded at depths from 651 to 1090 m in the Greenland Sea (Whatley et al. 1996); however, further investigation would be premature until taxonomic revisions of *Eucytherura* species (e.g., Horne and Lord in press) have progressed. It is unlikely that there are any bioluminescent podocopid ostracods. But, the possibility that bioluminescence of other deep-sea organisms (Warrant and Locket 2004; Birk et al. 2018; Martini et al. 2019) affects twilight-zone or deep-sea ostracods cannot be excluded, while there is no such evidence known so far. We also compared eye index values directly to the light availability data (PAR (*z*)), finding significantly more ostracod species with eye tubercles in higher light availability (PAR (*z*)) sites (Fig. 6; Table 1). The eye index values show a latitudinal gradient with higher values in lower latitudes (Figs. 1, 7), which can be partly explained by depth and light penetration, as the high central Arctic Ocean consists of deep basins and is covered by sea ice most of the year.

A noisy relationship between the eye index and depth and light availability (Figs. 3, 6) could have various reasons. Highly variable eye index values even in very shallow depths of almost zero could, at least in part, be because of the presence of sighted but eye-tubercle-less species that are known to be common (Tanaka 2005). We speculate that variable contributions of blind ostracods or those lacking eye tubercles in very shallow water can reflect variable relative abundance of infaunal vs. epifaunal taxa, for example, depending on substrate types, assuming less need of eyes in infaunal taxa. Another factor for highly variable light penetration in very shallow waters is spatiotemporally changing turbidity along the coast due to input of suspension through rivers and highly turbulent waters bringing additional sediment into suspension. The input of nutrients into the water column triggers higher plankton productivity as well in coastal proximity, thus further diminishing light penetration to the bottom.

In our study, there are seven sample sites with >0 eye index values located in water deeper than 1000 m, while their eye index values are low (Fig. 3). These nonzero eye index values in deeper depths are likely because of down-slope transportation of eyed-species shells. Most specimens recorded in the Arctic Ostracode Database are dead shells, which could be influenced by postmortem down-slope transportation and/or ice rafting by sea ice and icebergs. The shells at such sites are a

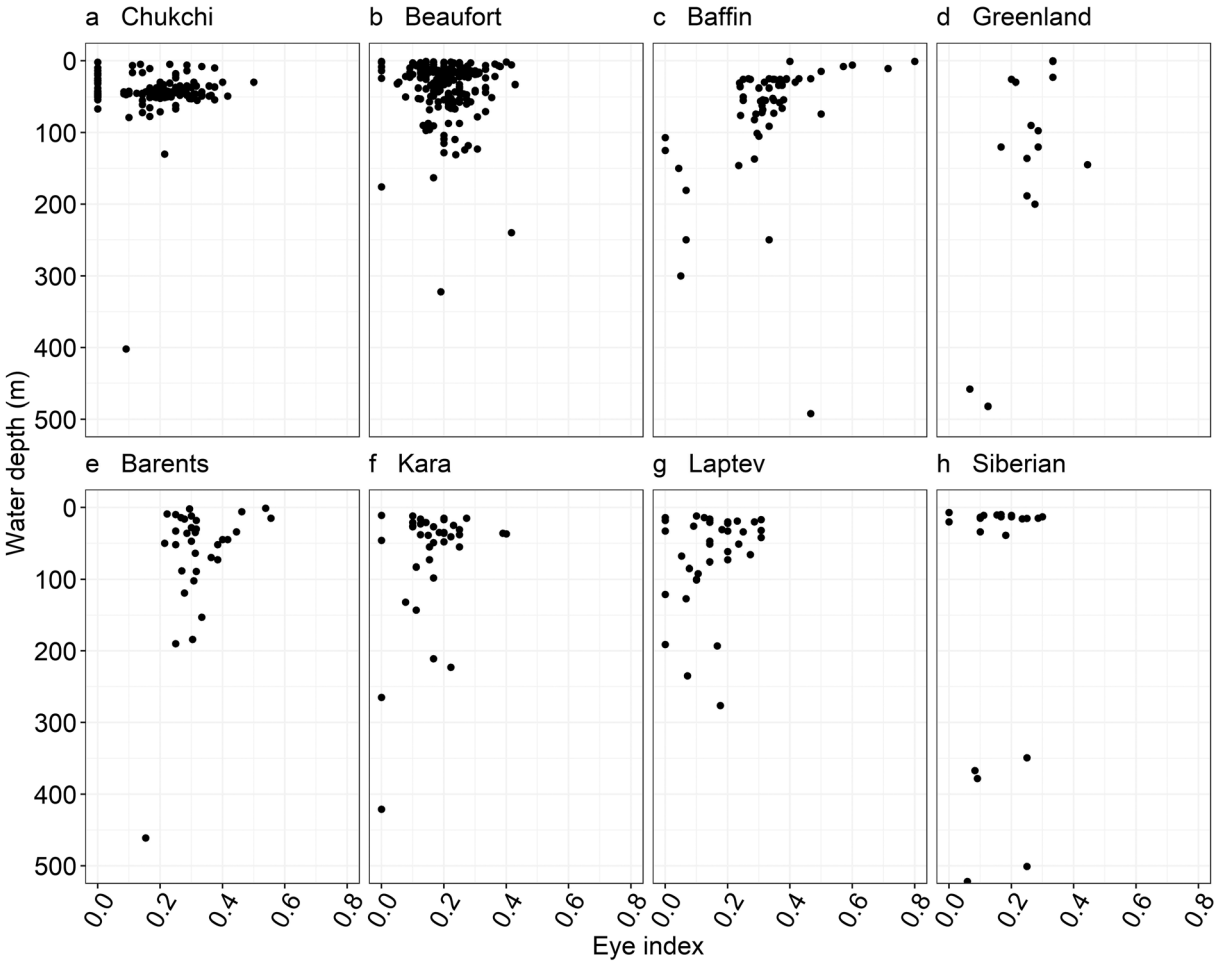

Fig. 4. Bathymetric distribution of eye index values in different regions (**a–h**) of the Arctic Ocean. Only samples from the top 500 m range are presented to show the regional difference of eye index values in shallow water among the various Arctic Ocean coastal seas.

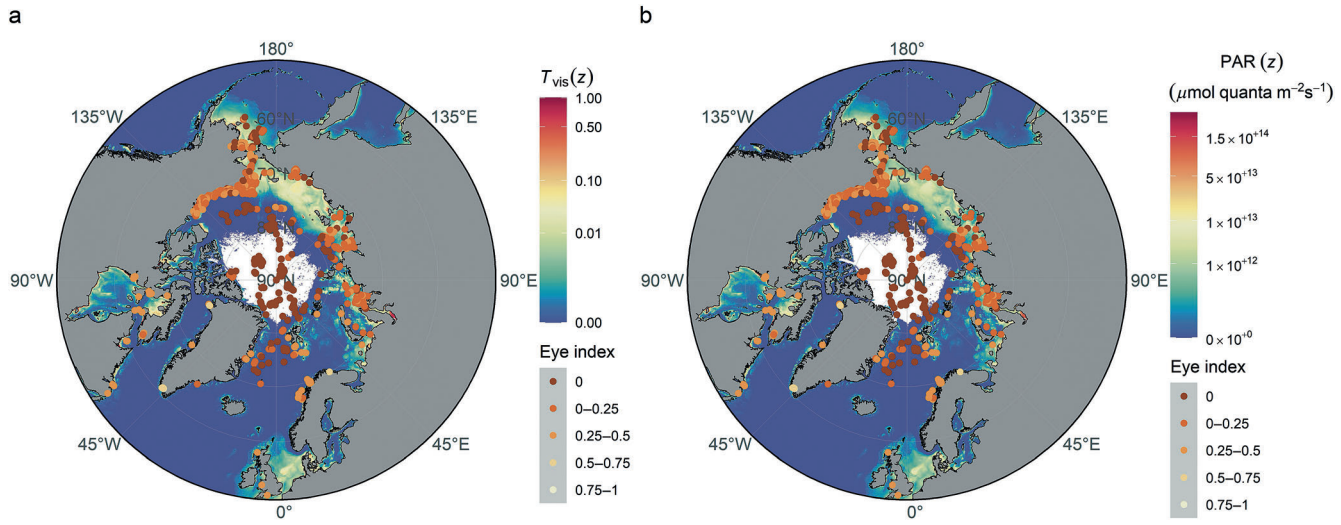

Fig. 5. Geographical distribution of light availability proxies. Heat maps indicate (**a**) vertical transmittance (T_{vis} (z)) and (**b**) photosynthetically available radiation at sampling depth (PAR (z)). Note that for sites in the high Arctic the white background indicates where the ocean color data were absent from the MODIS Aqua, potentially due to permanently ice-covered sites. Eye index values are shown on the maps.

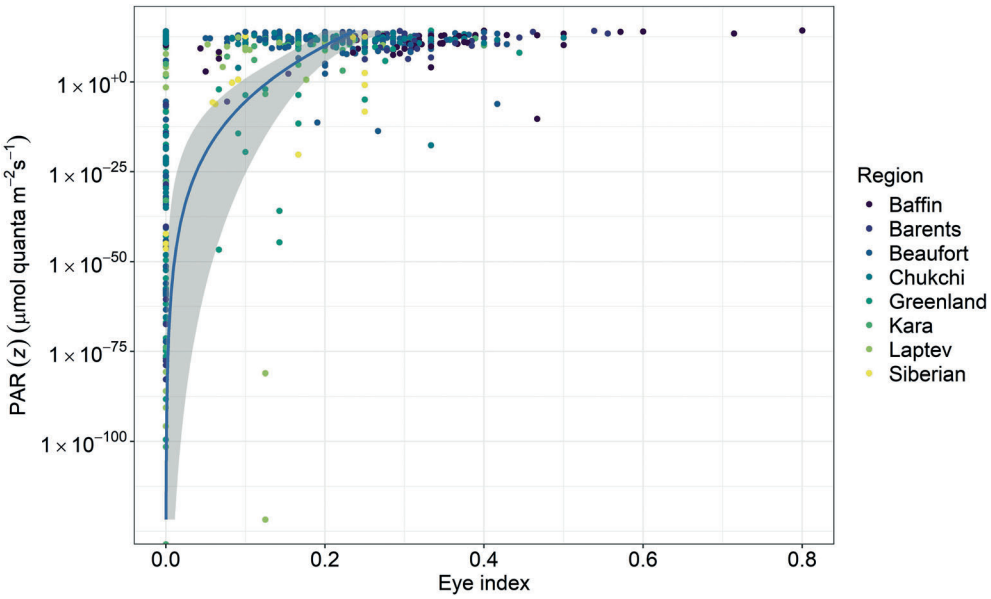

Fig. 6. Eye index and light availability proxy of the photosynthetically available radiation at sampling depth (PAR (*z*)). The blue lines show significant relationships with 95% confidence intervals (shaded area) based on GLMM with binomial distribution.

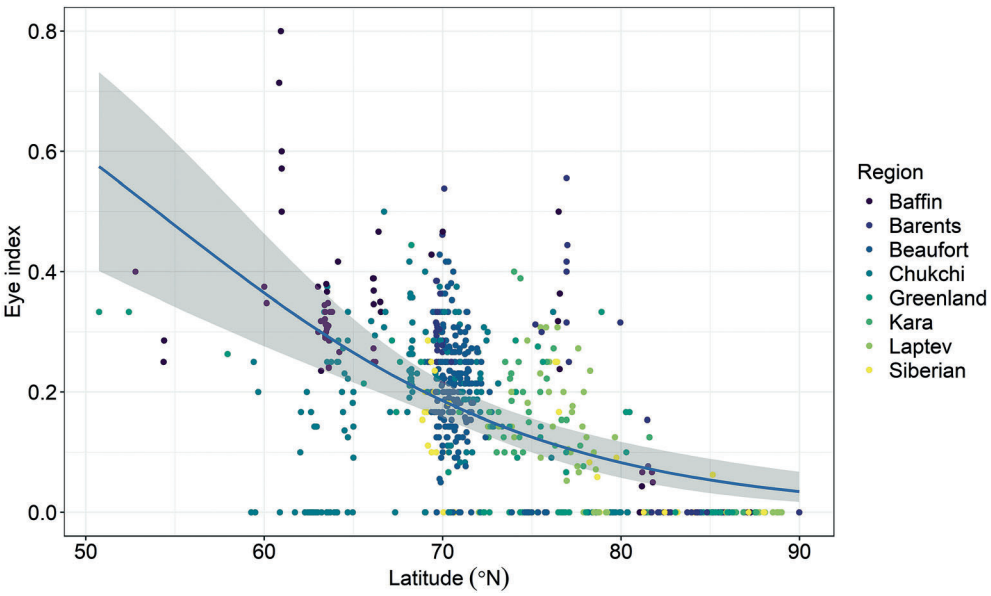

Fig. 7. Latitudinal gradient of eye index. The blue line shows significant relationship with 95% confidence intervals (shaded area) based on GLMM with binomial distribution.

combination of a small number of eye tubercle-bearing species and a large number of eyeless species. Eye tubercle-bearing species in those samples include *Muellerina abyssicola*, *Rabilimis mirabilis*, *Rabilimis septentrionalis*, *Roundstonia globulifera*, and *Thaerocythere crenulata*. They are primarily shallow-marine species and the abundance of these species is much higher in the shallow continental shelf /slope regions than in the deep sea (e.g., Zhang et al. 2022), suggesting that these shells are mainly transported down slope or ice-rafted postmortem.

The regional plots show the eye index peak in mid depths (~ 50 m), for example, in Chukchi, Kara, and Laptev Seas (Fig. 4). This could be explained, perhaps, from a functional perspective: as an external structure of the nauplius eye, the eye tubercle acts as a lens and strengthens sunlight passing

Table 1. GLMMs with binomial distribution on the eye index. The GLMMs were conducted using water depth, photosynthetically available radiation at depth (PAR (*z*)), or latitude as a fixed factor. Ocean regions (Fig. 1b) were used as the random factor in all three GLMMs.

	Estimate	Std. error	*z*-value	*p*-value
(Intercept)	−2.000	0.614	−3.254	0.0011
Depth	−0.153	0.062	−2.458	0.0140
(Intercept)	−6.203	0.807	−7.687	0.0000
PAR (*z*)	0.361	0.075	4.840	0.0000
(Intercept)	8.622	4.254	2.027	0.0427
Latitude	−0.194	0.065	−3.006	0.0026

through, so as light availability is adequate near the surface, a lens that further amplifies light for the eye is unnecessary. Although we are not sure if this could explain completely the appearance of low eye index values and species without eye tubercles in very shallow water depths, it is supported by evidence that relative eye tubercle sizes of modern podocopid ostracods increase as water depth increases from 0 to about 60 m and then decrease in deeper regions (i.e., ostracod eye sensitivity [= tubercle sizes] increases to compensate decreasing light availability until certain threshold) (Tanaka et al. 2009). High eye index variability of almost zero light availability (PAR (*z*)) sites (Fig. 6) could be explained by both the above-discussed postmortem transport and the necessity of vision enhancement in the twilight zone. Indeed, the light availability (PAR (*z*)) values are already very low in depths > 20 m (Fig. 8), supporting the idea of the vision enhancement necessity. Another issue is that the photosynthetically available radiation at depth (PAR (*z*)) cannot be accurately estimated below the well-mixed surface layer, as the vertical distribution of optical properties cannot be measured by satellite sensors (Lee et al. 2005). Nevertheless, despite the questionable accuracy of the absolute photosynthetically available radiation at depth (PAR (*z*)) values, they still indicate relative light conditions at depth. Similarly, it is difficult to estimate the photosynthetically available radiation at depth (PAR (*z*)) for permanently sea-ice-covered sites. However, permanently ice-covered sites are mostly in deep basins where eye index values are mostly zero (Fig. 1) and, thus, may not affect our results.

Our computation on the eye index assumes that the presence/absence of eye tubercles in a species illustrated in the literature is representative of all records of that species in the Arctic Ostracode Database. This assumption is necessary for us to apply data from the Arctic Ostracode Database and other similar census databases in the future when specimens are not available. The usage of species as a unit, rather than specimen, leads to a potential risk if individuals of a given species have eyes (eye tubercles) in shallow water but not in the deep sea. However, there is no such case so far reported, while there is no doubt that the relative size of the eye tubercle varies with the depth of the water and most, if not all, such cases known are interspecific (*see* Benson 1975, 1976; Tanaka et al. 2009). Similarly, we assume that the presence/absence of eye tubercles determined for a species represents 100% of specimens of that species in any given sample. Again, we have no evidence against this assumption, but it could be checked in a future study by examining even just a few assemblages containing multiple specimens of certain species (the higher the number, the more reliable the result), counting those with and those without eye tubercles, particularly at depths across the 600–800 m depth range proposed by Benson (1975) as being where eye tubercles disappear. It is also necessary to confirm that the eye tubercles in both left and right valves of individuals of a given species are equally developed; however, it is usual to see symmetric eye tubercle development in both valves (e.g., *see* scanning electron microscopic images in Yasuhara and Irizuki 2001) and there is no strong asymmetric case (e.g., eye tubercle present in right valve but absent in left valve) as far as we know. In addition, an important caveat is that, as mentioned in the introduction section, the presence of eye tubercles means sighted for sure, but absence of eye tubercles does not necessarily mean blind. Species without eye tubercles could still have eyes in their soft body. So, our eye index reconstruction could be underestimated (as it is lower than that of isopods; Fig. 3), since shallow depths could have sighted species without eye tubercle. Nonetheless, we believe that our eye-tubercle-based study is the best practical approach with the advantage of utilizing a large existing census dataset, allowing it to cover large spatial and bathymetrical ranges with a large sample size, and providing a good approximation, given the current limitation of available data and biological knowledge on ostracod eyes and vision.

The depth of visible light penetration in the ocean varies with latitude and seasonally, being deeper in low latitudes and shallower in polar waters (Menzies et al. 1968; Thurston and Bett 1993). The daily maximum angle of incidence of sunlight on the water surface varies with latitude and season; at high latitudes more sunlight is reflected by the ocean surface than at low latitudes, so that less light penetrates the water. Another important factor at high latitudes is the attenuation of light by seasonal or perennial sea ice (Laney et al. 2017). The influence of prolonged winter darkness in polar regions is also likely to be significant. However, it must be borne in mind that depth distributions may also be explicable in terms of other environmental factors, key among which is water temperature; the apparent correlation of the poleward emergent distributions of abyssal isopod genera with light penetration depth may be coincidental and their occurrences better explained by their adaptation to low temperatures (Menzies et al. 1968). Indeed, the eye index shows significant negative relationship with latitude in this study (Fig. 7; Table 1). However, in the Arctic Ocean, higher latitudes are

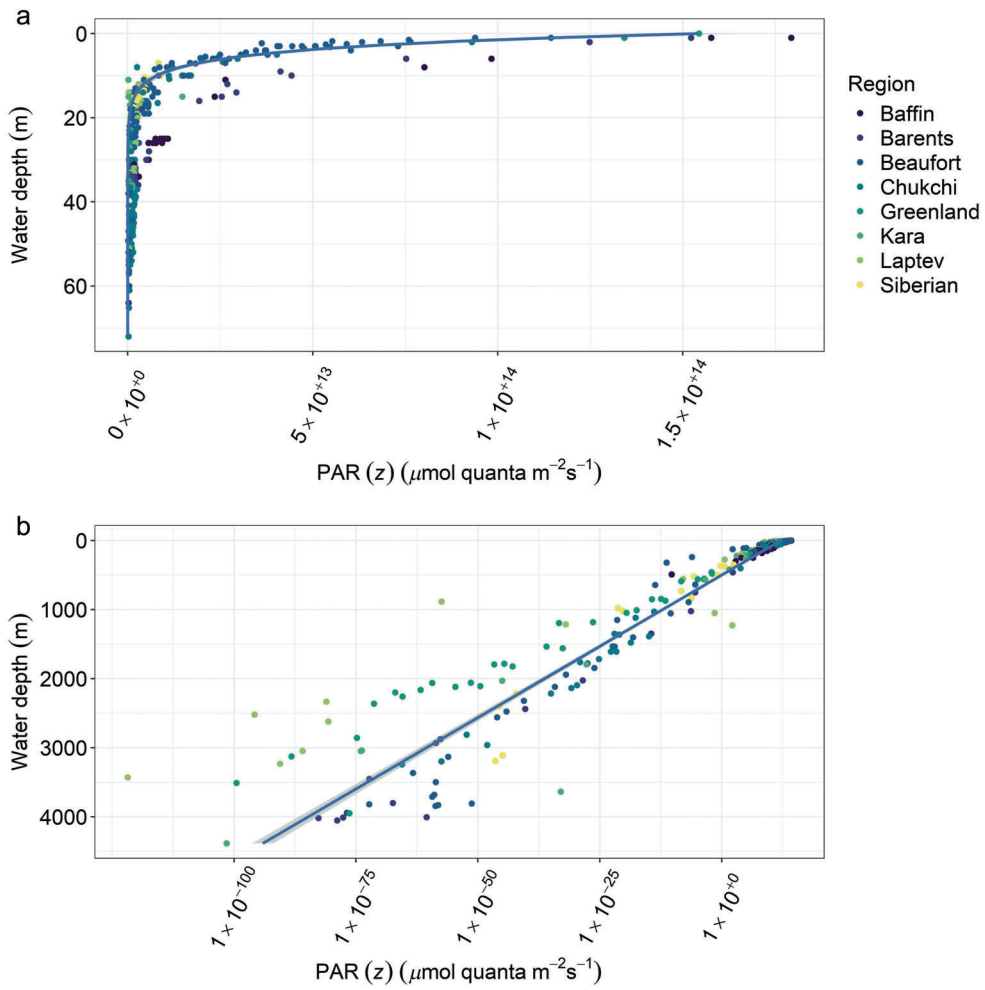

Fig. 8. Photosynthetically available radiation at sampling depth (PAR (z)) as functions of water depth: (**a**) for the top 70 m; (**b**) for the full bathymetric range. The blue line shows significant relationship with 95% confidence intervals (shaded area) based on GLMM with Gaussian distribution and logarithmic link function. Data with the vertical transmittance T_{vis} (z) less than 0.1% (along with the photosynthetically available radiation at sampling depth, PAR(z)) were removed before conducting GLMM.

deeper and latitude and water depth are highly correlated ($r = 0.68$). Thus, it is uncertain if latitude (more correctly environmental factors driven by latitude) affects ostracode vision in the Arctic Ocean.

Conclusion

Eye loss with increasing depth and decreasing light is at least common in multiple crustacean groups as well as some gastropods, and the trend could be quantitatively similar among various deep-sea organisms. It is worth noting that relatively deep depths with reduced light still have eyed species. This may be because limited light requires good vision, as demonstrated by mesopelagic fishes in twilight zones which have eyes that "tend to be large" (Salvanes and Kristoffersen 2001, p. 1714). Indeed, ostracod eye-tubercle size is known to be larger not in shallowest depths but in an intermediate depth of ~ 50 m (Tanaka et al. 2009). Our quantitative reconstruction of the relationship between "eye" and water depth and light availability throughout the Arctic Ocean is an important baseline for broader research on vision in the ocean macroecologically (and macroevolutionarily, given ostracods' excellent fossil records including eye tubercles as a part of fossilized hard parts), that was enabled by the massive census compilation effort of the Arctic Ostracode Database and recent development of satellite-based observations.

Data availability statement

All data and code are available in Zenodo open data repository (Zhang et al. 2024; https://doi.org/10.5281/zenodo.10786211) and NOAA's National Centers for Environmental

Information (NCEI) (https://www.ncdc.noaa.gov/paleo/study/32312).

References

Alvarez Zarikian, C. A. 2015. Cenozoic bathyal and abyssal ostracods beneath the oligotrophic South Pacific Gyre (IODP Expedition 329 Sites U1367, U1368 and U1370). Palaeogeogr., Palaeoclimatol. Palaeoecol. **419**: 115–142. doi:10.1016/j.palaeo.2014.07.024

Anderson, A., and D.-E. Nilsson. 1981. Fine structure and optical properties of an ostracode (Crustacea) nauplius eye. Protoplasma **107**: 361–374. doi:10.1007/BF01276836

Benson, R. H. 1975. Morphologic stability in Ostracoda. Bull. Am. Paleontol. **65**: 13–46.

Benson, R. H. 1976. The evolution of the ostracode *Costa* analysed by "Theta-Rho difference" (discussion), p. 127–139. *In* G. Hartmann [ed.], Evolution of post-Palaeozoic Ostracoda: Abhandlungen und Verhandlungen des Naturwissenschaftlichen Vereins in Hamburg. (NF) 18/19 (Suppl.). L. Friederichsen.

Benson, R. H. 1984. Estimating greater paleodepths with ostracodes, especially in past thermospheric oceans. Palaeogeogr. Palaeoclimatol. Palaeoecol. **48**: 107–141. doi:10.1016/0031-0182(84)90093-2

Benson, R. H., R. M. Del Grosso, and P. L. Steineck. 1983. Ostracode distribution and biofacies, Newfoundland continental slope and rise. Micropaleontology **29**: 430–453. doi:10.2307/1485518

Birk, M. H., M. E. Blicher, and A. Garm. 2018. Deep-sea starfish from the Arctic have well-developed eyes in the dark. Proc. R. Soc. B Biol. Sci. **285**: 20172743. doi:10.1098/rspb.2017.2743

Cronin, T. M., L. Gemery, W. M. Briggs, M. Jakobsson, L. Polyak, and E. M. Brouwers. 2010. Quaternary Sea-ice history in the Arctic Ocean based on a new Ostracode sea-ice proxy. Quat. Sci. Rev. **29**: 3415–3429.

Cronin, T. M., and others. 2021. NOAA/WDS paleoclimatology—Arctic Ostracode Database 2020 (AOD2020). doi:10.25921/grn9-9029

Danielopol, D. L., A. Baltanäs, and G. Bonaduce. 1996. The darkness syndrome in subsurface-shallow and deep-sea dwelling Ostracoda (Crustacea). Biosyst. Ecol. Ser. **11**: 123–143.

Denton, E. J. 1990. Light and vision at depths greater than 200 metres, p. 127–148. *In* P. J. Herring, A. K. Campbell, M. Whitfield, and L. Maddock [eds.], Light and life in the sea. Cambridge Univ. Press.

Freiwald, A., and N. Mostafawi. 1998. Ostracods in a cold-temperate coastal environment, Western Troms, northern Norway: Sedimentary aspects and assemblages. Facies **38**: 255–273. doi:10.1007/BF02537368

Gemery, L., and others. 2017. An Arctic and Subarctic ostracode database: Biogeographic and paleoceanographic applications. Hydrobiologia **786**: 59–95. doi:10.1007/s10750-015-2587-4

Horne, D. J., and A. R. Lord. in press. The ostracod genus *Eucytherura* G.W. Müller and the "*Cythere complexa* Brady" problem. *PalZ*.

Kaji, T., and A. Tsukagoshi. 2010. Heterochrony and modularity in the degeneration of maxillopodan nauplius eyes. Biol. J. Linn. Soc. **99**: 521–529.

Kontrovitz, M., and J. J. H. Myers. 1988. Ostracode eyes as paleoenvironmental indicators: Physical limits of vision in some podocopids. Geology **16**: 293–295. doi:10.1130/0091-7613(1988)016<0293:OEAPIP>2.3.CO;2

Laney, S. R., R. A. Krishfield, and J. M. Toole. 2017. The euphotic zone under Arctic Ocean sea ice: Vertical extents and seasonal trends. Limnol. Oceanogr. **62**: 1910–1934. doi:10.1002/lno.10543

Lee, Z., K. Du, R. Arnone, S. C. Liew, and B. Penta. 2005. Penetration of solar radiation in the Upper Ocean: A numerical model for oceanic and coastal waters. J. Geophys. Res. **110**: C09019. doi:10.1029/2004JC002780

Mackiewicz, A. 2006. Recent benthic Ostracoda from Hornsund, south Spitsbergen, Svalbard Archipelago. Pol. Polar Res. **27**: 71–90.

Martini, S., L. Kuhnz, J. Mallefet, and S. H. Haddock. 2019. Distribution and quantification of bioluminescence as an ecological trait in the deep sea benthos. Sci. Rep. **9**: 14654.

Menzies, R. J., R. Y. George, and G. Rowe. 1968. Vision index for isopod Crustacea related to latitude and depth. Nature **217**: 93–95. doi:10.1038/217093a0

Mikko, V. 2020. PlotSvalbard: PlotSvalbard—plot research data from Svalbard on maps. Institute of Marine Research, Available from https://mikkovihtakari.github.io/PlotSvalbard/articles/PlotSvalbard.html

Müller, G. W. 1894. Die Ostracoden des Golfes von Neapel und der angrenzenden Meeres-Abschnitte. Fauna Flora Golfes von Neapel **21**: 1–404.

Neale, J. W., and H. V. Howe. 1975. The marine Ostracoda of Russian harbor Novaya Zemlya and other high latitude faunas. Bull. Am. Paleontol. **65**: 381–417.

Niven, J. E., and S. B. Laughlin. 2008. Energy limitation as a selective pressure on the evolution of sensory systems. J. Exp. Biol. **211**: 1792–1804. doi:10.1242/jeb.017574

Okada, R., A. Tsukagoshi, R. J. Smith, and D. J. Horne. 2008. The ontogeny of the platycopid *Keijcyoidea infralittoralis*. (Ostracoda: Podocopa). Zool. J. Linn. Soc. **153**: 213–237. doi:10.1111/j.1096-3642.2008.00383.x

Penney, D. N. 1993. Northern North Sea benthic Ostracoda: Modern distribution and palaeoenvironmental significance. Holocene **3**: 241–254. doi:10.1177/095968369300300306

Porter, M. L., and L. Sumner-Rooney. 2018. Evolution in the dark: Unifying our understanding of eye loss. Integr. Comp. Biol. **58**: 367–371. doi:10.1093/icb/icy082

R Core Team. 2020. R: A language and environment for statistical computing. R Foundation for Statistical Computing, Available from http://www.R-project.org

Raupach, M. J., C. Mayer, M. Malyutina, and J. Wägele. 2009. Multiple origins of deep-sea Asellota (Crustacea: Isopoda) from shallow waters revealed by molecular data. Proc. R. Soc. B Biol. Sci. **276**: 799–808. doi:10.1098/rspb.2008.1063

Salvanes, A., and J. B. Kristoffersen. 2001. Mesopelagic fishes, p. 1711–1717. *In* K. Turekian, S. A. Thorpe, and J. Steele [eds.], Encyclopedia of ocean sciences, v. **3**. Academic Press.

Schornikov, E. I., and M. A. Zenina. 2006. FEB RAS Marine Investigations in the Arctic. *In* Proceedings of the Arctic Regional Center, vol. 4. Vladivostok: Dalnauka. ISBN 5-8044-0684-1.

Smith, R., and T. Kamiya. 2014. The freshwater ostracod (Crustacea) genus *Notodromas* Lilljeborg, 1853 (Notodromadidae) from Japan; taxonomy, ecology and lifestyle. Zootaxa **3841**: 239–256. doi:10.11646/zootaxa.3841.2.4

Stepanova, A. 2006. Late Pleistocene-Holocene and recent Ostracoda of the Laptev Sea and their importance for paleoenvironmental reconstructions. Paleontol. J. **40**: S91–S204. doi:10.1134/S0031030106080016

Sumner-Rooney, L. 2018. The kingdom of the blind: Disentangling fundamental drivers in the evolution of eye loss. Integr. Comp. Biol. **58**: 372–385. doi:10.1093/icb/icy047

Sumner-Rooney, L., J. D. Sigwart, J. McAfee, L. Smith, and S. T. Williams. 2016. Repeated eye reduction events reveal multiple pathways to degeneration in a family of marine snails. Evolution **70**: 2268–2295. doi:10.1111/evo.13022

Syme, A. E., and T. H. Oakley. 2012. Dispersal between shallow and abyssal seas and evolutionary loss and regain of compound eyes in cylindroleberidid ostracods: Conflicting conclusions from different comparative methods. Syst. Biol. **61**: 314–336. doi:10.1093/sysbio/syr085

Tanaka, G. 2005. Morphological design and fossil record of the podocopid ostracod naupliar eye. Hydrobiologia **538**: 231–242.

Tanaka, G. 2006. Functional morphology and light-gathering ability of podocopid ostracod eyes and the palaeontological implications. Zool. J. Linn. Soc. **147**: 97–108.

Tanaka, G., D. J. Siveter, and A. R. Parker. 2009. The visual system and paleoecology of the Silurian ostracod *Primitiopsis planifrons*. J. Paleo. **83**: 414–421. doi:10.1666/08-124.1

Thurston, M. H., and B. J. Bett. 1993. Eyelessness in marine gammaridean Amphipoda (Crustacea): Geographical, bathymetric and taxonomic considerations. J. Nat. Hist. **27**: 861–881. doi:10.1080/00222939300770531

Tsukagoshi, A., R. Okada, and D. J. Horne. 2006. Appendage homologies and the first record of eyes in platycopid ostracods, with the description of a new species of *Keijcyoidea* (Crustacea: Ostracoda) from Japan. Hydrobiologia **559**: 255–274. doi:10.1007/s10750-005-1139-8

Warrant, E. J., and N. A. Locket. 2004. Vision in the deep sea. Biol. Rev. **79**: 671–712. doi:10.1017/S1464793103006420

Whatley, R., M. Eynon, and A. Moguilevsky. 1996. The depth distribution of Ostracoda from the Greenland Sea. J. Micropalaeontol. **17**: 15–32.

Whatley, R. C., and M. P. Eynon. 1996. Four new Arctic deep-water ostracod species from East Greenland, p. 195, 23–200, 27. *In* M. C. Keen [ed.], Proceedings of the 2nd European Ostracodologists' meeting. University of Glasgow.

Wickham, H. 2016. ggplot2: Elegant graphics for data analysis. Springer-Verlag, Available from: https://cran.r-project.org/web/packages/ggplot2/index.html

Williams, S. T., E. S. Noone, L. M. Smith, and L. Sumner-Rooney. 2022. Evolutionary loss of shell pigmentation, pattern, and eye structure in deep-sea snails in the dysphotic zone. Evolution **76**: 3026–3040. doi:10.1111/evo.14647

Yasuhara, M., and T. Irizuki. 2001. Recent Ostracoda from the northeastern part of Osaka Bay, southwestern Japan. J. Geosci. Osaka City Univ. **44**: 57–95.

Yasuhara, M., H. Okahashi, and T. M. Cronin. 2009. Taxonomy of quaternary deep-sea ostracods from the western north Atlantic ocean. Palaeontology **52**: 879–931. doi:10.1111/j.1475-4983.2009.00888.x

Yasuhara, M., A. Stepanova, H. Okahashi, T. M. Cronin, and E. M. Brouwers. 2014. Taxonomic revision of deep-sea Ostracoda from the Arctic Ocean. Micropaleontology **60**: 399–444. doi:10.47894/mpal.60.5.01

Yasuhara, M., G. Hunt, H. Okahashi, and S. N. Brandão. 2015. Taxonomy of deep-sea Trachyleberidid, Thaerocytherid, and Hemicytherid genera (Ostracoda). Smithson. Contrib. Paleobiol. **96**: 1–216.

Yasuhara, M., H. Okahashi, H. M. Huang, Y. Hong, H. Iwatani, R. W. C. Chu, and G. Hunt. 2021. Quaternary equatorial Atlantic deep-sea ostracodes: Evidence for a distinct tropical fauna in the deep sea. J. Paleo. **95**: 1–41. doi:10.1017/jpa.2021.52

Zhang, J., and others. 2024. Sight and blindness: The relationship between eyes, water depth, and light availability in the Arctic Ocean. (v1.2.0) [Data set]. Zenodo. doi:10.5281/zenodo.10786211

Zhang, P., and others. 2022. Southward migration of Arctic Ocean species during the last glacial period. Geophys. Res. Lett. **49**: e2022GL100818. doi:10.1029/2022GL100818

Acknowledgments

We thank Rachel P.P. Wong for continuous support; Gene Hunt, Dan L. Danielopol, and Maria Karpuk for helpful and constructive comments and discussion; editors Thomas Kiørboe and K. David Hambright and two anonymous reviewers for helpful and thoughtful comments. The work described in this article was partially supported by grants from the Research Grants Council of the Hong Kong Special Administrative Region, China (project codes: RFS2223-7S02, G-HKU709/21). C.-L.W. was funded by the National Science and Technology Council, Taiwan (NSTC 112-2611-M-002-011). T.M.C. and L.G. were funded by the US Geological Survey, Climate Research and Development Program. Any use of trade, firm, or product names is for descriptive purposes only and does not imply endorsement by the US Government.

Conflict of Interest

None declared.

Submitted 10 November 2023
Revised 09 March 2024
Accepted 21 April 2024

Associate editor: Thomas Kiørboe